Indian Journal of Pure & Applied Physics
Vol. 45, March 2007, pp. 231-237

Structural and magnetic properties of zinc ferrite aluminates

[#]Roshan Lal, Suman, N D Sharma, S P Taneja* & V R Reddy**

Department of Physics, Kurukshetra University, Kurukshetra 136 119

*Department of Physics, Maharshi Dayanand University, Rohtak 124 001

**UGC-DAE Consortium for Scientific Research, Khandwa Road, Indore 452 017

Received 28 October 2005; revised; 4 August 2006; accepted 4 January 2007

Zinc ferrite aluminates $ZnAl_xFe_{2-x}O_4$ with composition ($0 \leq x \leq 1$) were synthesized at 1150°C using the usual ceramic method and studied by X-ray diffraction, magnetization and Mössbauer measurements. It is observed that lattice parameter decreases, with increasing Al concentration (x). Mössbauer absorption spectra of all the samples recorded at room temperature showed three hyperfine magnetic sextets and a single quadrupole doublet. The outer sextet is assigned to α- Fe_2O_3 crystalline phase, whereas inner two sextets refer to Fe^{3+} ions at octahedral (B) site and tetrahedral (A) site showing the formation of zinc ferrite aluminates phase. The hyperfine magnetic field was found to decrease with increasing Al concentration and has been explained on the basis of super transferred hyperfine field. The central doublet is partially dissociated forming $ZnFeO_2$ (delafossite) phase overlapping the main Mössbauer spectra measured at room temperature. The observed variations in saturation magnetization in all the samples have been explained on the basis of site distribution and the strength of the exchange interactions between the magnetic ions. On the basis of these observations, it is concluded that the present ferrite system exhibits a non-collinear magnetic structure with a very weak ferromagnetic character, which starts dominating further when zinc ferrite is diluted with non-magnetic Al^{3+} ions.

Keywords: Structural properties, Magnetic properties, Zinc ferrite aluminates, X-ray diffraction, Mössbauer absorption spectra

IPC Code: G01J3/28

1 Introduction

Zinc ferrite in bulk form has the normal spinel structure and falls in the class of soft magnetic materials, which offer an excellent opportunity for its uses in electrical, semi-conductor, radio engineering, automatics and computer technology[1]. In the spinel structure, there are two different types of interstitial sites present, namely tetrahedral (A) and octahedral (B), which are occupied by different metal ions. The magnetic properties of the spinel ferrites arise from the ability of these compounds to distribute the metal ions among the available tetrahedral (A) and octahedral (B) sites. In general, the magnetic interactions between these metal ions, limited only to the nearest neighbours, are antiferromagnetic in nature and their magnitudes are given by exchange integrals. For example the exchange integral J_{AB} describes the nature and the strength of the interaction between any two nearest A and B ions. Similarly, J_{AA} and J_{BB} are the exchange integrals showing the strength of A-A and B-B nearest neighbour interactions. The advantage of the mixed spinel has been considered *i.e.* all the interactions are well defined for the nearest neighbour, and are antiferromagnetic, with $|J_{AA}| \gg |J_{BB}| \gg |J_{AA}|$. When the two sub-lattices (A and B) are occupied by the magnetic ions of the same type, then the A-B inter-sublattice interactions represented by exchange integral J_{AB} are much greater than B-B and A-A intra-sublattice interactions. Thus the moments on A and B sites are aligned anti-parallel to each other and the spins have a collinear structure. However, when one of the intra-sublattice interactions becomes comparable with the inter-sublattice interaction it leads to a non-collinear spin structure[2]. It is well known that when the ferrites are sufficiently diluted with non-magnetic ions they can show a wide spectrum of magnetic order ranging from ferromagnetic, antiferromagnetism, local canting spin (LCS) to semi-spin glass and glass[3]. Extensive work has been reported regarding the impurity substitution in the different ferrites system in order to improve their basis properties[4-6]. In the present work,

[#]E-mail: roshandhiman_kuk@yahoo.co.in

we have studied the effect of Al^{3+} substitution on the magnetic properties of zinc ferrites using X-ray, Mössbauer and magnetization measurements.

2 Experimental Details

2.1 Sample preparation

The samples of the solid solution series $ZnAl_xFe_{2-x}O_4$ for x = 0.0,0.2,0.4,0.8 and 1.0 were prepared by standard ceramic method. The starting materials were AR grade zinc oxide, aluminium oxide and iron oxide with 99.3% purity supplied by S D fine India. The chemicals were weighed in required proportion and mixed. The samples were ground, palletized and pre-sintered at 1000°C in air atmosphere for 24 h. In the final sintering process, the samples were placed in a furnace at 1150°C for 24 h in air and then slowly cooled to room temperature at the rate of 2°C/min.

2.2 X-ray measurements

The X-ray diffraction patterns were recorded sing Cu-Kα radiation (angle range 20-80°) on a Regaku X-ray dffractometer.

2.3 Magnetization measurements

The magnetization measurements (M versus H) of all samples were carried out at 300K using vibrating sample magnetometer (VSM). However M versus T for all the samples were carried out at the magnetic field of 30 Oe in the temperature range 87-300K.

2.4 Mössbauer measurements

Samples were crushed to obtain the fine powder and sieved through a 200 μm gauge. The absorption spectra were recorded in transmission geometry at room temperature with a constant acceleration Mössbauer derive. A single line ^{57}Fe(Rh) source with initial activity of 10 mCi was used. The Mössbauer spectrometer was calibrated using an enriched α-Fe foil. The experimental data were computer fitted using a NORMOS site program assuming Lorentzian line shape with χ^2 minimization technique. The solid line through the data points is the result of the computer fit of the data

3 Results and Discussion

3.1 X-ray measurements

In Fig. 1, the recorded X-ray diffraction patterns for all compositions of $ZnAl_xFe_{2-x}O_4$ system (x = 0.0,0.2,0.4,0.8 and 1.0) show all those lines, which belong to the cubic spinel structure. The

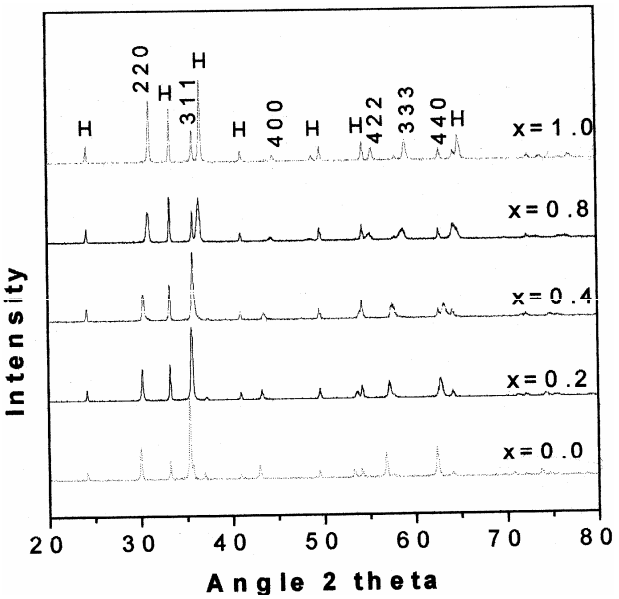

Fig. 1—Typical XRD patterns for $ZnFe_{2-x}O_4$ system; (x = 0.0, 0.2,.4,.8 & 1.0)

reflection from the planes (200), (311), (400), (422), (333) and (440) appears for all the samples.

The appearance of these planes proves that the present system have a cubic ferrite phase[7]. In addition to the ferrite phase, XRD also detected hematite (α-Fe_2O_3) The formation of second phase such as α-Fe_2O_3 is a consequence of the preferential loss of the divalent Zn ions during firing process, as Zn is more volatile and has low melting point[8]. It may be added that we have prepared the samples twice and got the similar results. These observations suggest that ZnO which helps in the formation of ferrite, is lost during firing process, however, the remaining amount of zinc oxide is not compatible for the complete conversion into ferrite phase[8]. A number of such defect spinel ferrites and the existence of such a structural phase comparable with α-Fe_2O_3 have been reported by researchers[9]. At lower aluminium concentration some of the ferrite and hematite peaks are superimposed while at higher concentration these peaks are well resolved, this is due to the fact that aluminium has higher melting point, causes incomplete conversion of Fe_2O_3 into ferrite phase. The interplanr distance d(Å) was calculated using Bragg's law and the values of lattice constant a (Å) were determined using the following relation:

$$a = d_{hkl}\,(h^2+k^2+l^2)^{1/2} \quad \ldots \quad (1)$$

and are shown in Table 1. The value of lattice constant a (Å) decreases linearly with increasing Al

Table 1—Lattice constant, X-ray density, saturation magnetization, magneton number for $ZnAl_xFe_{2-x}O_4$ system

Content x	Lattice constant	X-ray density (d_x)	σ_x (emu/gm) 300K	$\eta_B(\mu_B)$ 300K	Blocking Temperature T_B (K)
0.0	8.4041	5.3928	--	--	< 80
0.2	8.3398	5.3867	2.11	0.089	165
0.4	8.3044	5.3204	2.06	0.084	189
0.8	8.2234	5.2021	1.80	0.070	>300
1.0	8.1764	5.1511	1.22	0.046	>300

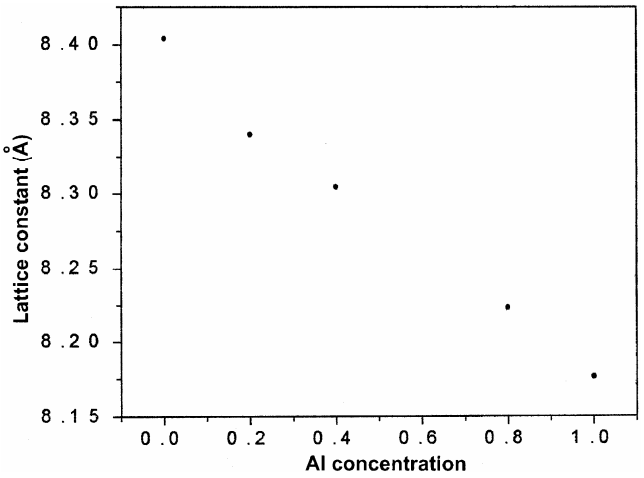

Fig. 2—Variation of lattice constant a (Å) with Al^{3+} concentration, x

content x as shown in Fig. 2. Thus, obeying the Vegard's law[10], which may be attributed to the replacement of larger Fe^{3+} ions (0.64 Å) by smaller Al^{3+} ions in the $ZnAl_xFe_{2-x}O_4$ system. The X-ray density (d_x) of each sample was calculated by the relation:

$$d_x = ZM/NV \quad \ldots \quad (2)$$

where Z is the number of molecules per unit cell (Z = 8), M the molecular weight, V the unit cell volume and N is Avogadro's Number. The X-ray density decreases with increasing aluminium concentration (x). This is because the decrease in mass overtakes the decrease in volume of the unit cell.

3.2 Magnetization measurements

A variation of magnetization with applied field at 300K is presented in Fig 3. The typical characteristic of a weak ferromagnetic behaviour *i.e.* a small hystersis loop with almost immeasurable coercivity and remanence is observed for the sample x = 0.0. However, for the other samples, saturation

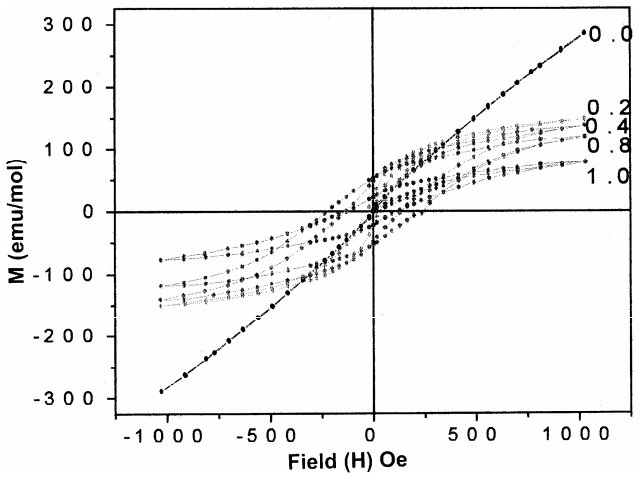

Fig. 3—Field dependence of magnetization curve at 300K for $ZnFe_{2-x}O_4$ system

magnetization was calculated by extrapolating the magnetization versus the inverse of the field curve to $1/H = 0$.

On addition of non-magnetic Al^{3+} ions in place of iron ions, the hystersis loop *i.e.* the ferromagnetic character starts dominating further. This is due to the fact that α-Fe_2O_3 has not completely changed into ferrite phase. Therefore, our X-ray results also show the existence of extra peaks of α-Fe_2O_3 in addition to the ferrite phase. To explain the composition dependence of magnetization in the ferrite system, the concept of cation distribution may also be taken into account. In spinel structure, each tetrahedral site is linked with 12 octahedral sites, while an octahedral site is linked with 6 tetrahedral sites through the strong super exchange interaction. So there is a combination of 12 nearest neighbours of a tetrahedral iron ion, consisting of two kinds of ions (Fe^{3+}, Al^{3+}) distributed randomly over octahedral sites. Then the possible cation distribution for the normal spinel can be represented as follows:

$$(Zn^{2+})[Fe^{3+}_{2-x}Al^{3+}_{x}]\ O_4 \quad \ldots \quad (3)$$

However, in the present system Fe_2O_3 is not completely converted into ferrite phase, and the presence of extra peaks of α-Fe_2O_3, the presence of extra peaks of α-Fe_2O_3, exhibit a magnetic structure, therefore the above-proposed cation distribution can also take the following form:

$$(Zn^{2+}_{1.0-z}\ Fe^{3+}_{\alpha}\ Al^{3+}_{\beta}\square_{\gamma})[Zn^{2+}_{z}\ Fe^{3+}_{2-x-\alpha}\ Al^{3+}_{x-\beta}\square_{x-\gamma}] \quad \ldots \quad (4)$$

where □ is a cation vacancy on the tetrahedral and the octahedral sites, that may be occupied by α-Fe_2O_3.

The saturation magnetization per formula unit in Bohr magneton $\eta_B(\mu_B)$ for all the samples was calculated from the hystersis loop data obtained at 300K by the following relation;

$$\eta_B(\mu_B) = M.Wt \times \sigma_s / 5585 \quad \ldots \quad (5)$$

The variation of η_B (the saturation magnetization per formula unit in Bohr magneton μ_B) was obtained from hystersis loop technique as a function of Al concentration and is shown in Table 1. From the field dependence of magnetization and the observed value of magnetic moments at room temperature, it is evident that the values of $\eta_B(\mu_B)$ decrease with increase in aluminium concentration (x) and is due to

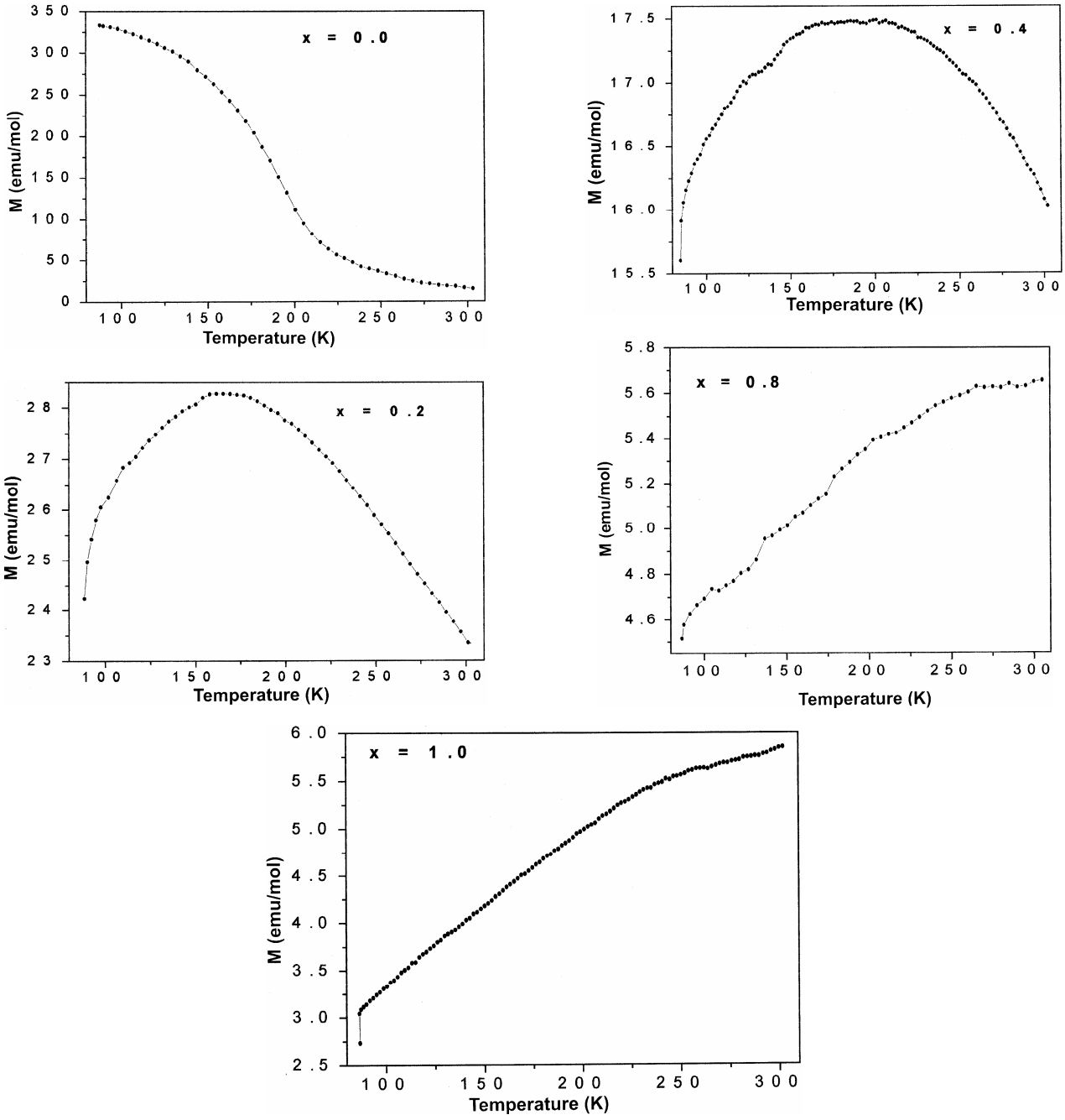

Fig. 4—Plots of magnetization against temperature (x = 0.0,.2,.4,0.8 & 1.0)

replacement of Fe^{3+} ions by non-magnetic Al^{3+} ions [11]. Observation of the extra peaks that corresponds to α-Fe_2O_3 phase would also contribute towards the reduction of magnetization[8] along with the mechanism discussed above. The variation of magnetization with temperature at the applied field of 30 Oe is shown in Fig. 4 (x = 0.0 to 1.0)

It is observed that blocking temperature increases with increasing Al^{3+} concentration. Below blocking temperature ferrite exhibits a hystersis feature[12]. It is clear from Fig. 4(a) that is for x = 0.0, zinc ferrite aluminates exhibits a small hystersis loop indicating a very weak ferromagnetic character. On further increasing the Al^{3+} concentration the blocking temperature increases as a result the hystersis loop *i.e.* the ferromagnetic character starts dominating further. Finally, at x = 1.0, the sample exhibits a clear hystersis loop.

3.3 Mössbauer measurements

Mössbauer absorption spectra for all the samples i.e. x = 0.0,0.2,0.4,0.8 and 1.0 were recorded at room temperature as shown in Fig. 5. The spectra were computer fitted and the hyperfine parameters are presented in Table 2. The Mössbauer spectra exhibit a broad asymmetric sextet along with a central doublet as shown in Fig. 5. The central doublet in all the samples arises due to the presence of non-magnetic zinc ions [13-15] as well as incomplete oxidation of hematite into ferrite phase[16]. All the spectra were fitted with three sextets and single quadrupole doublet. Because of overlap in the sextets, one has to use the constraint of line widths. The outer most sextet is attributed to crystalline component *i.e.* α-Fe_2O_3 phase, whereas inner sextets, are due to the Fe^{3+} ions at the octahedral (B) site and the other due to the Fe^{3+} ions at the tetrahedral (A) site. It is well known that Zn^{2+} has marked preference only for tetrahedral (A) sites, whereas iron and aluminium ions co-exist at both A and B-sites, however, they prefer the B-sites. On increasing the aluminium concentration, the outer most sextet becomes more intense as compared to the other two sextets, this shows that ferrite was not formed in a single phase, which is also reflected in our X-ray studies. As the aluminium concentration is increased, the paramagnetic doublet decreases indicating a reduction of the $ZnFeO_2$ (delafossite) phase[17-18], similar results have also been observed in copper ferrite aluminaes[18]. The value of isomer shift of Fe^{3+} ions the tetrahedral (A) and octahedral (B) sites, listed in Table 1 showed no significant change, which indicates that s-electron density at the Fe^{3+} nucleus, is not affected by Al^{3+} substitution. In the present system, the value of the magnetic hyperfine field decreases with increasing Al^{3+} ion concentration (x) in $ZnAl_xFe_{2-x}O_4$ system. The decrease in the value of H_{hf} with x can be explained on the basis of Neel's molecular field

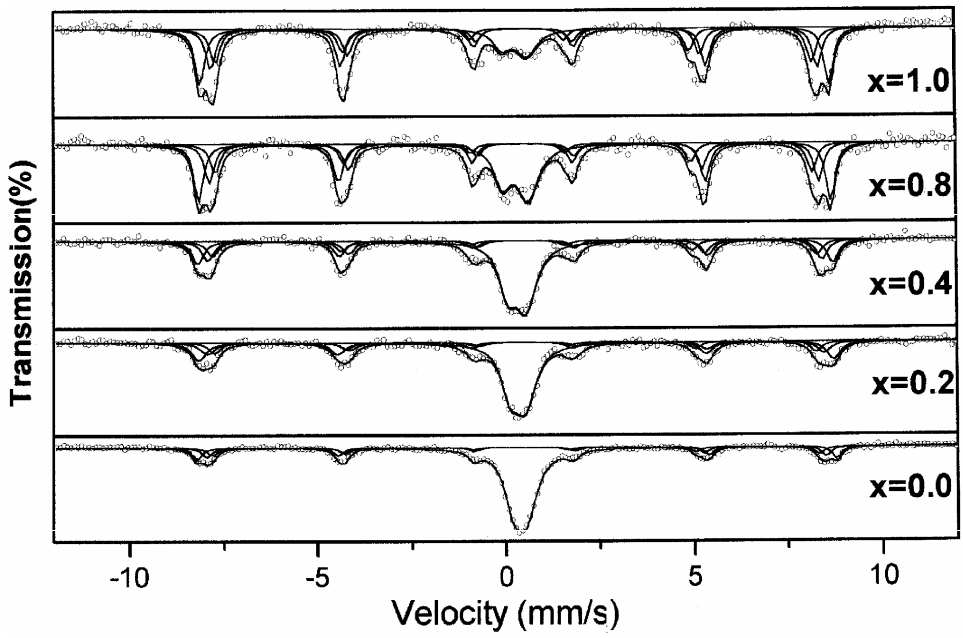

Fig. 5—Mössbauer absorption spectra recorded at 300K for $ZnFe_{2-x}O_4$ system; (x = 0.0, 0.2, 0.4, 0.8 and 1.0)

Table 2—Hyperfine interaction parameters computed from the Mossbauer absorption spectra recorded at room temperature, isomer is given relative to α-Fe

Content x	Site	I S ($\delta \pm 0.01$) mm/s	Q S ($\Delta \pm 0.01$) mm/s	Area (%)	H_{int} ± 2.0 T
0.0	H	0.37	–0.19	14.09	52.7
	B	0.38	–0.22	11.22	51.0
	A	0.30	–0.11	09.32	50.0
	D	0.34	0.35	65.37	---
0.2	H	0.35	–0.17	24.38	52.3
	B	0.40	–0.32	15.77	50.8
	A	0.32	–0.14	11.72	49.6
	D	0.30	0.40	48.13	---
0.4	H	0.36	–0.22	27.21	52.2
	B	0.40	–0.31	17.93	50.6
	A	0.27	–0.05	14.50	49.4
	D	0.28	0.48	40.36	---
0.8	H	0.35	–0.19	33.16	52.0
	B	0.38	–0.30	22.54	50.2
	A	0.27	–0.09	17.22	49.2
	D	0.25	0.65	27.08	---
1.0	H	0.37	–0.23	36.01	51.9
	B	0.38	–0.26	26.83	50.1
	A	0.24	–0.06	22.23	49.0
	D	0.24	0.67	14.93	---

theory and super transferred hyperfine field mechanism. The super transferred hyperfine field at Fe^{3+} ion at the B-site is due to spin transfer from the d-orbitals of the nearest-neighbour cations which occupy the B-site through the ligand anions to the s–orbital of the Fe^{3+}(A) ion. Thus, the super transferred hyperfine field at the A-site will depend on the magnetic moment of the B-site. Due to the site preference, the Al^{3+} ions prefer the B-sites and the substitution of Fe with the non-magnetic Al^{3+} ions, results in replacing Fe ions from A and B-sites simultaneously. This causes the reduction in magnetization at the both sites, which in turn reduced the super transferred hyperfine field. Such a variation can be explained qualitatively, zinc ferrite ($ZnFe_2O_4$) in the bulk form has normal spinel structure in which divalent (Zn^{2+}) ions occupy A-sites, allow only B-B interaction[19]. On addition of Al^{3+} ions in place of iron ions, Al^{3+} ions have got a strong tendency to occupy B-site, it reduces AB interaction with increase in aluminium concentration. As the aluminium concentration is increased, the BB super transferred hyperfine interactions become comparable in strength because of canting of spins (non-collinear). These BB super transferred hyperfine interactions are strongly dependent on the spins and therefore, reduce the net hyperfine field[20-21]. It is also evident from the Mössbauer absorption spectra that there is a systematic decrease in the internal magnetic hyperfine field H_{hf} values with the increasing aluminium substitution. This happens because the replacement of larger Fe^{3+} ions (0.64Å) by smaller Al^{3+} (0.51Å) ions influence the internal hyperfine fields at the nearest Fe^{3+} sites through transferred hyperfine fields. The result observed in the present study is that the intensity and the area of all the three sextets increase, however the area of the paramagnetic doublet corresponds to $ZnFeO_2$ (delafossite) phase decreases on increasing non-magnetic Al^{3+} ions concentration. Such observations suggest that the ferromagnetic character increases on increasing Al^{3+} ions concentration.

4 Conclusion

The system $ZnAl_xFe_{2-x}O_4$ (x = 0.0) shows a very weak ferromagnetic behaviour. The magnetic behaviour dominates further *i.e*. the system shows clear hystersis loop when the value of x approaches to 1.0. The values of magnetic moment per formula unit in Bohr magneton obtained from M/H curve decreases with increasing Al^{3+} concentration and hence showing the similar trend. These results are also in good agreement with our Mössbauer measurements. Mössbauer studies also show that there exists a $ZnFeO_2$ delafossite phase beside the main matrix $ZnAl_xFe_{2-x}O_4$. It is thus, concluded that a non-collinear magnetic structure exists and the complete formation of ferrite phase does not occur in the present system.

Acknowledgement

The authors are grateful to Dr N P Lalla and Dr Alok Banerji, Scientist, UGC-DAE, Consortium for Scientific Research, Indore, for their help in carrying out XRD and magnetization measurements respectively.

References

1 Oliver S A, Harris V G, Hamdeh H H & Ho J C, *Appl Phys Lett*., 76, 19 (2000) 2761.
2 Yafet Y & Kittal C, *Phys Rev B,* 87 (1952) 290.
3 Dramann J I & Nogus M, *J Phys: Condens Matter,* 2 (1990) 1223.
4 Parvatheeswara Rao B, Subha Rao P S V & Rao K H, *IEEE Trans Magn,* 33, 6 (1997) 4454.
5 Das A R, Ananthan V S & Khan D C, *J Appl Phys,* 57 (1985) 4189.

6 Ata-Allah S S & Fayek M K, *J Phys Chem Solids*, 61 (2000) 1529.

7 Amer M A, *Phys Stat Sol* (a) 181 (2000) 539.

8 Chander Rath, Anand S, Das R P, Kulkarni S D, Date S K & Mishra N C, *J Appl Phys*, 91, 4 (2002) 2211.

9 Lee Sung Ho & Kim Woong Tae, *J Phys: Condens Matter*, 4 (1992) 8245.

10 Winfrey C G, Eckort D W & Tauber A, *J Am. Chem Soc*, 82 (1960) 2695.

11 Mundada O G, Modi Kunal B, Jadhav K M, & Bichile G K, *Indian J of Pure & Appl. Phys*, 35 (1997) 554.

12 Kale A, Gubbala S & Mishra R D K, *J Magn Magn Matter*, 277 (2004) 350.

13 Thumber K P, Chhantbar M C, Modi K B, Baldha G J & Joshi H H, *J Magn Magn Mater*, 280 (2004) 23.

14 Modi Kunal B, Joshi H H and Kulkarni R G, *Indian J of Pure & Appl. Phys*, 34 (1996) 92.

15 Yang De Ping, lavoie Lindsey K, Zhang Yide, Zhang Zongalo and Shinhui Ge, *J Appl Phys,* 93, 10 (2003) 7492.

16 Das Dipankar, *Indian J Phys*, 78 A 2 (2004) 185.

17 Kulkarni R G, Trivedi Bimal S, Joshi H H and Baldha G J, *J Magn Magn Mater*, 159 (1996) 375.

18 Almokhtar M, Abdalla Atef M, Gaffar M A, *J Magn Magn Mater*, 272- 276 (2004) 2216.

19 Greenwood N N & Gibb T C, *Mössbauer spectroscopy*, Chapman and Hall Ltd. London (1971).

20 Srivastava M C, Shringi S N & Srivastava R G, *Phys Rev B*, 14 (1976) 2041.

21 Rao A D P, Raju S B, Vadera S R & Sharma D R, *Bull Mater Sci*, 26, 5 (2003) 505.

Figure Caption

Fig. 1—Typical XRD patterns for $ZnFe_{2-x}O_4$ system; (x = 0.0, 0.2,.4,.8 & 1.0)

Fig. 2—Variation of lattice constant a (Å) with Al^{3+} concentration, x

Fig. 3—Field dependence of magnetization curve at 300K for $ZnFe_{2-x}O_4$ system

Fig. 4—Plots of magnetization against temperature (x = 0.0,.2,.4,0.8 & 1.0)

Fig. 5—Mössbauer absorption spectra recorded at 300K for $ZnFe_{2-x}O_4$ system; (x = 0.0, 0.2, 0.4, 0.8 and 1.0)

Table 1—Lattice constant, X-ray density, saturation magnetization, magneton number for $ZnAl_xFe_{2-x}O_4$ system

Content x	Lattice constant	X-ray density (d_x)	σ_x (emu/gm) 300K	$\eta_B(\mu_B)$ 300K	Blocking Temperature T_B (K)
0.0	8.4041	5.3928	--	--	< 80

0.2	8.3398	5.3867	2.11	0.089	165
0.4	8.3044	5.3204	2.06	0.084	189
0.8	8.2234	5.2021	1.80	0.070	>300
1.0	8.1764	5.1511	1.22	0.046	>300

Table 2—Hyperfine interaction parameters computed from the Mossbauer absorption spectra recorded at room temperature, isomer is given relative to α-Fe

Content x	Site	I S (δ±0.01) mm/s	Q S (Δ±0.01) mm/s	Area (%)	H_{int} ± 2.0 T
0.0	H	0.37	–0.19	14.09	52.7
	B	0.38	–0.22	11.22	51.0
	A	0.30	–0.11	09.32	50.0
	D	0.34	0.35	65.37	---
0.2	H	0.35	–0.17	24.38	52.3
	B	0.40	–0.32	15.77	50.8
	A	0.32	–0.14	11.72	49.6
	D	0.30	0.40	48.13	---
0.4	H	0.36	–0.22	27.21	52.2
	B	0.40	–0.31	17.93	50.6
	A	0.27	–0.05	14.50	49.4
	D	0.28	0.48	40.36	---
0.8	H	0.35	–0.19	33.16	52.0
	B	0.38	–0.30	22.54	50.2
	A	0.27	–0.09	17.22	49.2
	D	0.25	0.65	27.08	---
1.0	H	0.37	–0.23	36.01	51.9
	B	0.38	–0.26	26.83	50.1
	A	0.24	–0.06	22.23	49.0
	D	0.24	0.67	14.93	---